



Spent mushroom: a new low-cost adsorbent for removal of Congo Red from aqueous solutions

Xiuli Tian^a, Chuang Li^a, Huaijin Yang^b, Zhixiang Ye^b, Heng Xu^{a,*}

^aKey Laboratory for Bio-resources and Eco-environment of Education Ministry, College of Life Science, Sichuan University, Chengdu 610064, China

Tel. +86 28 85414644; email: xuheng64@sina.com

^bCollege of Resources and Environment, Chengdu University of Information Technology, Chengdu 610100, China

Received 29 June 2010; Accepted 17 August 2010

ABSTRACT

In this study, spent mushroom (SM) (*Tricholoma lobayense*) was used as a new low-cost adsorbent for removing Congo Red (CR) from aqueous solutions in a batch process at 25 °C. By varying the adsorbent dose, initial concentration, contact time, initial pH and particle size, the respective effects of these factors on the adsorption performance were explored. The sorption equilibrium data fitted Langmuir isotherm and the maximum adsorption capacity was 147.1 mg/g at 25 °C. The kinetic data obtained at different initial concentrations were analyzed using pseudo-first-order, pseudo-second-order and intraparticle diffusion equations. The pseudo-second-order described the adsorption of Congo Red on spent mushroom very well.

Keywords: Spent mushroom; Congo Red; Adsorption; Isotherm; Kinetics

1. Introduction

Textile printing and dyeing is one of major industries in China and produces large volumes of wastewater during the preprocessing and dyeing processes. It is reported that the discharge volumes of these wastewater reaches 14.13×10^8 tons per year [1]. Some dyes are carcinogenic and mutagenic and are toxic to the aquatic life and the food web [2]. Therefore, the removal of such colored agents from aqueous effluents is of significant environmental, technical, and commercial importance [3].

Currently, a number of methods have been developed for the removal of dyes from wastewaters to decrease their damage to the environment. The technologies involve adsorption on inorganic or organic matrices, decolorization by photocatalysis, and/or by oxidation processes, microbiological or enzymatic decomposition, etc. [4]. Among these removal technologies, adsorption

is considered to be an effective method due to the ease of operation and comparable low cost of application. At present, the most commonly used adsorbent in wastewater treatment is activated carbon, which has also been studied for the dye removal. But the extensive application of activated carbon is still in difficulty due to its high cost. Therefore, it is necessary to explore cheaper adsorbent for wastewater treatment. Some researchers have reported many low-cost materials which are mainly from industrial and agricultural production, such as broad bean peels [5], spent tea leaves [6], fly ash [7], wheat straw [8], bagasse fly ash [9], pomelo (*Citrus grandis*) peel [10], clinoptilolite [11], Ca-bentonite [12], rice husk [13], Jute stick powder [14], almond shells [15], groundnut shell [16], activated palm ash [17].

Tricholoma lobayense is a precious edible mushroom, which is extensively grown in south China. Spent *T. lobayense* is a waste in the process of mushroom production, which includes stipes of mushroom and sub-quality ones. Due to the high consumption of *T. lobayense*, massive

*Corresponding author.

amounts of the spent *T. lobayense* (as waste) are disposed, causing a severe problem in the environment. Hence, the utilization of such waste is most desirable. Furthermore, after adsorption of dyes, the spent *T. lobayense* can also be used for biogas production. Congo Red (CR) is an anionic dye, which has been widely used in textiles, paper, rubber and plastic industries [18]. The aim of this study was to investigate the potential of spent *T. lobayense*, an abundantly available solid waste, as a low-cost adsorbent in the removal of an anionic dye, Congo Red (CR), from aqueous solutions.

2. Materials and methods

2.1. Adsorbate

Congo Red (CR) used in this study was of analytical grade chemicals (C.I. = 22,120, chemical formula = $C_{32}H_{22}N_6Na_2O_6S_2$, FW = 696.7, $\lambda_{max} = 500$ nm) and was purchased from Kelong Chemical Reagent Factory, Cheng du, Sichuan province, China. The structure of CR is shown in Fig. 1.

2.2. Preparation of adsorbent

Fresh spent edible mushroom (*T. lobayense*) was collected from a mushroom production site near Chengdu, Sichuan. Prior to use, it was cleaned and the sample was then air dried and boiled with water until the filtered water was cleared. After being dried at 50 °C for 24 h, it was then powdered using a grinder. Then it was passed through 60 mesh, 100 mesh and 200 mesh (< 75 μ m) sieve and stored in a plastic bottle for further use. No other chemical or physical treatment was used prior to adsorption experiments.

2.3. Preparation of dye solution and estimation

Stock solutions (1000 mg/l) of CR was prepared in double distilled water and diluted to get the desired concentration of the dyes. Concentrations of dyes were determined by finding out the absorbance at the characteristic wavelength using UV/vis spectrophotometer. Before all the experiment, calibration curves for the

dyes should be prepared by measuring the absorbance of different concentrations of the dyes at their optimum λ_{max} using UV/vis spectrophotometer. The dye concentrations in calibration curves were controlled within 30 mg/l. Therefore, the samples with higher concentrations of CR (> 30 mg/l) were diluted with distilled water to make the concentration less than 30 mg/l. Amount of dye uptake, q (mg/g), was calculated using the following equation:

$$q = (C_i - C_f) \cdot V / 1000 W \quad (1)$$

where C_i (mg/l) is the initial dye concentration, C_f (mg/l) is the dye concentration after adsorption, W (g) is the amount of adsorbent and V (l) is the volume of the solution.

2.4. Adsorption experiments

To study some important parameters like adsorbent dose, initial concentration, contact time, pH and particle size, each batch experiments was performed in a 150 ml stoppered glass Erlenmeyers flasks containing a definite volume (50 ml in each flask) at 25 °C on a constant temperature breeding shaker (SUKUN) with a shaking of 180 rpm. After adsorption, all the samples were centrifuged at 10,000 rpm for 5 min and analyzed for the residual dye concentration. The effect of spent mushroom dose on the amount of CR adsorbed was studied by adding different amounts (0.05 g, 0.10 g, 0.20 g, 0.40 g, 0.60 g, 0.80 g, and 1.00 g). The effect of initial pH on dye removal was studied over a pH range of 2–12. The pH was adjusted by the addition of diluted aqueous solutions of HCl or NaOH (0.10 M). To study the adsorption isotherms, adsorption experiments were carried out by adding 0.2 g sorbent into 50 ml of different initial concentrations (80–450 mg/l) dye solution without changing the solution pH. For adsorption kinetics, the procedures were basically identical to those of equilibrium tests. The samples were taken at different time intervals for analyzing the residual dye concentration. The effect of particle size on dye removal was conducted by adding different particle size adsorbent (60 mesh, 100 mesh and 200 mesh) into 50 ml 100 mg/l dye solution. All the experiments were conducted in duplicate. Besides, two controls were performed. A blank, 50 ml of the dye solution without any sorbent was shaken. A control, with only the adsorbents in 50 ml of double-distilled water was also shaken to determine any color leaching of the adsorbent.

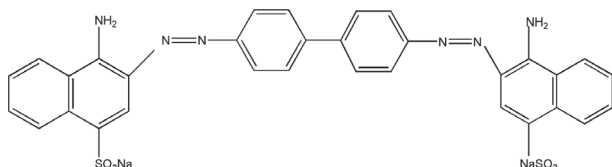


Fig. 1. Molecular structure of Congo Red.

3. Results and discussion

3.1. Effect of adsorbent dose on dye adsorption

The effects of adsorbent dose on the %removal of CR are shown Fig. 2. It was observed that the %removal

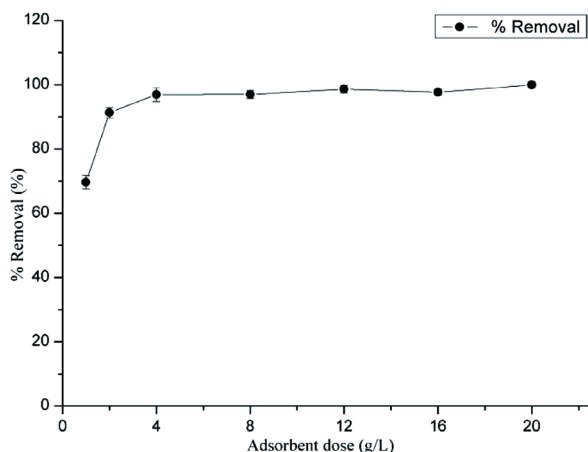


Fig. 2. Effect of adsorbent dosage on the adsorption of CR on SM (temperature = 25 °C, $C_0 = 100$ mg/l, stirring rate = 180 rpm, equilibrium time = 1 h).

increased with increasing in adsorbent dose. At equilibrium time of 1 h, the %removal increased from 69.66% to 100% for an increase in SM dose from 0.05 to 1.00 g. Above 4 g/l of sorbent dose, the adsorption equilibriums of dyes reached and the %removal of dyes was almost unchanged. So, optimum SM dose was found to be 4 g/l. The increase in %removal of CR was due to the increase of the available sorption surface and availability of more adsorption sites. A similar observation was previously reported for removal of methylene blue from aqueous solution by spent tea leaves [6].

3.2. Effect of initial pH

The effect of initial solution pH on the %removal of CR at equilibrium conditions is shown in Fig. 3. It was observed

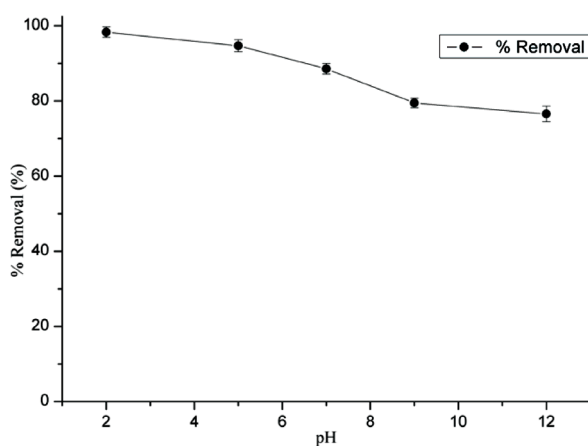


Fig. 3. Effect of solution pH on the adsorption of CR on SM (temperature = 25 °C, $C_0 = 100$ mg/l, stirring rate = 180 rpm, equilibrium time = 1 h).

that the %removal decreased with increasing solution pH. The removal rates were the highest at pH 2 (98.34%) and the lowest at pH 12 (76.60%). The q_e decreased from 24.59 mg/g to 19.15 mg/g while pH increased from 2 to 12.

Several reasons may be attributed to the dye adsorption behavior of the adsorbent at different solution pH, such as the active sites and the charge of surface of SM, and the chemical property of solution at different pH. At lower pH, the surface of adsorbent may be positively charged, while the solution ions were negatively charged, so the electrostatic attraction was the main force between the adsorbent and anionic dye. At higher pH, the surface of adsorbent particles may be negative charged, the main force was electrostatic repulsion and resulted in the decreased removal rates. Also, there was competition between OH^- (at higher pH) and colored ions of CR for positively charged adsorption sites. Similar results were reported in the literature [19–21].

3.3. Effect of adsorbent particle size

The effects of adsorbent particle size on the %removal of CR and q_e are shown in Table 1. It can be seen that both %removal of CR and q_e increased with the decrease in adsorbent particle size. The reason that can account for this is the surface area of adsorbent, which increases with the decrease in adsorbent particle size and can provide more active sites for dye adsorption. Similar observations were also reported by other investigators [5,22].

3.4. Adsorption kinetics

Effect of contact time and initial CR concentration on adsorption of CR by SM are shown in Fig. 4. As shown in Fig. 4, with increasing C_0 from 80 to 450 mg/l, the amount of CR adsorbed per unit mass of adsorbent increased from 19.40 to 99.90 mg/g, although the removal rate decreased from 96.86% to 88.75%. The C_0 provides the necessary driving force to overcome the resistances to the mass transfer of CR between the aqueous and the solid phases and enhances the interaction between adsorbate and adsorbent. It was observed that equilibrium time were different for different initial concentrations. The equilibrium conditions were reached

Table 1

CR removal percentages of different particle size (dye concentration: 100 mg/l; sorbent dose: 4 g/l; contact time: 1 h; pH 5.0; stirring rate = 180 rpm)

Particle size (mesh)	CR removal (%)	q_e (mg/g)
60	81.27	20.32
100	91.53	22.88
200	92.75	23.19

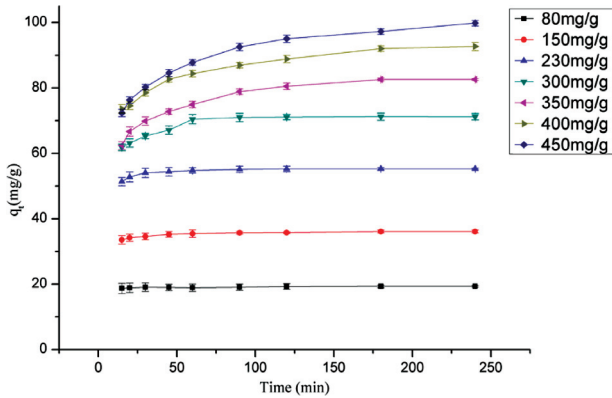


Fig. 4. Effect of contact time and initial concentration on the adsorption of CR on SM.

within 30–60 min for initial concentrations less than 300 mg/l while 180 min was needed for concentrations from 350 to 450 mg/l. From the above observation, it is evident that for lower initial concentration of the dye, the adsorption is very fast and equilibrium time is shorter. For various adsorbents, the equilibrium times are very different. For example, Bulut et al. [23] reported that after 60 min, the amount of CR adsorbed reached equilibrium for initial concentration from 75 to 300 mg/l at 25 °C. Other authors [24] reported that the amount of dye adsorbed (mg/g) by coir pith carbon reached

equilibrium after 10 min for the dye concentrations 20, 40, 60 and 80 mg/l at 35 °C.

In order to investigate the mechanism of adsorption, pseudo-first-order, pseudo-second-order and the intraparticle diffusion model were used to study the kinetics of adsorption of CR on SM.

3.4.1. Pseudo-first-order model

The pseudo-first-order model is described by Lagergren as [25]:

$$\log (q_e - q_t) = \log q_e - k_1 t / 2.303 \tag{2}$$

where q_e (mg/g) is the amount of CR adsorbed at equilibrium, q_t (mg/g) is the amount of CR adsorbed at time t and k_1 (1/min) is the rate constant of pseudo-first-order adsorption. k_1 and q_e are calculated from the slopes and intercepts of plots of $\log (q_e - q_t)$ versus t .

The values of parameters of three kinetic models and the determination factor (R^2) are presented in Table 2. It can be seen that the R^2 for pseudo-first-order model are not very high [0] in all initial CR concentrations, varying from 0.8676 to 0.9592. Also, the q_e calculated from pseudo-first-order model were very low compared with experimental q_e . This suggested that it was not appropriate to use pseudo-first-order model to predict the adsorption kinetics of CR onto SM.

Table 2
Kinetic parameters for the removal of Congo Red by SM ($T = 298$ K, $C_0 = 80, 150, 230, 300, 350, 400, 450$ mg/l)

C_0 (mg/l)	$q_{e,exp}$ (mg/l)	Pseudo-first-order model			Pseudo-second-order model		
		k_1 (min ⁻¹)	$q_{e,cal}$ (mg/l)	R^2	k_2 (q/mg min) ⁴	$q_{e,cal}$ (mg/l)	R^2
80	19.40	0.0156	1.0380	0.9592	0.0645	19.41	1.000
150	36.10	0.0352	5.2905	0.9337	0.0219	36.23	1.000
230	55.30	0.0267	3.9801	0.8676	0.0172	55.56	1.000
300	71.30	0.0256	0.9742	0.8916	0.0059	71.94	0.9999
350	82.62	0.0352	42.6481	0.9269	0.0021	84.75	0.9998
400	92.71	0.0285	40.7380	0.9072	0.0021	94.34	0.9995
450	99.90	0.0228	3.3767	0.9011	0.0014	102.04	0.9993

Intraparticle diffusion model

C_0 (mg/l)	$k_{id,1}$ (mg/g min ^{1/2})	I_1	$(R_1)^2$	$k_{id,2}$ (mg/g min ^{1/2})	I_2	$(R_2)^2$	$k_{id,3}$ (mg/g min ^{1/2})	I_3	$(R_3)^2$
150	1.6012	27.254	0.9740	0.1326	34.256	0.8342	–	–	–
230	2.9131	39.808	0.9871	0.1184	53.674	0.8165	–	–	–
300	3.9274	45.642	0.9055	2.1288	53.525	0.9758	0.1011	9.795	0.8263
350	5.699	40.904	0.9954	2.2312	57.71	0.9995	0.4759	75.583	0.7924
400	5.3551	52.027	0.9104	3.0364	61.516	0.9745	0.9937	77.887	0.9457
450	7.8094	41.946	0.9905	3.0581	63.801	0.9963	1.049	83.454	0.9913

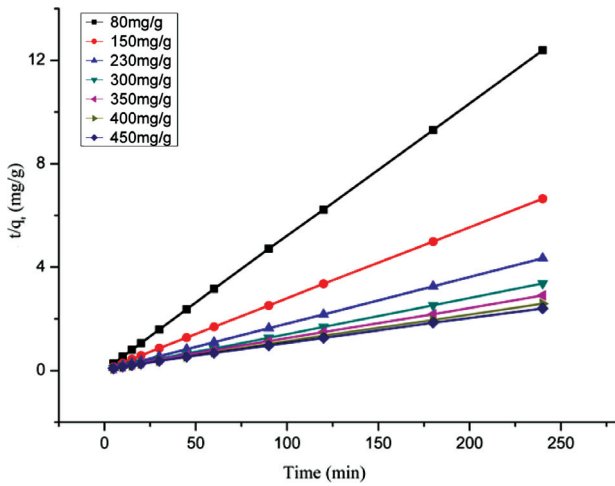


Fig. 5. The fitting of pseudo-second-order model for CR on SM for different initial concentrations at 25 °C.

3.4.2. Pseudo-second-order model

The pseudo-second-order kinetics can be expressed as [26]:

$$t/q_t = 1/k_2q_e^2 + t/q_e \quad (3)$$

where k_2 (g/mg min) is the rate constant of pseudo-second-order adsorption, q_t (mg/g) is the amount of CR adsorbed at time t , k_2 and q_e are calculated from the slopes and intercepts of plots of t/q_t versus t .

The plots of the linearized form of the pseudo-second-order kinetic model for adsorption of CR on SM are shown in Fig. 5. It can be seen from Table 2 and Fig. 5 that the determination factors were extremely high, in the range of 0.9993–1. Compared with pseudo-first-order model, the q_e calculated from pseudo-second-order kinetic model for all concentrations were very close to experimental q_e . Therefore, the adsorption of CR follows second-order kinetics. A similar result was reported for the adsorption of CR from aqueous solution onto Ca-bentonite [12].

3.4.3. Intraparticle diffusion

The intraparticle diffusion equation is given by the following equation [27]:

$$q_t = k_{id} t^{1/2} + I \quad (4)$$

where q_t (mg/g) is the amount of CR adsorbed at time t , k_{id} (mg g⁻¹ min^{-1/2}) is the intra-particle diffusion rate constant and I is the intercept, which are obtained from the slope of the straight line of q_t versus $t^{1/2}$.

Intraparticle diffusion is a possible rate-limiting step in adsorption system. The intraparticle diffusion plots of

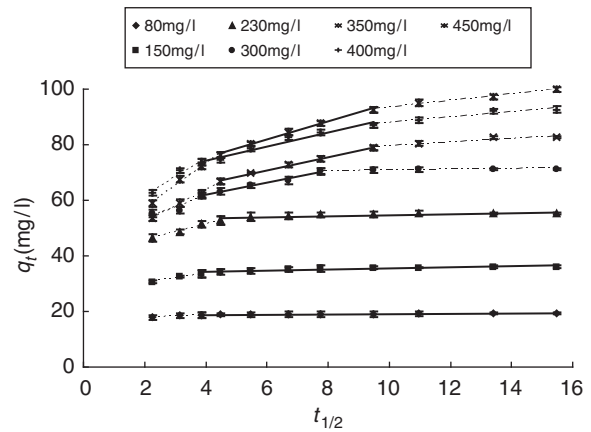


Fig. 6. Intraparticle diffusion plots for CR adsorption on SM for different initial concentrations at 25 °C.

the experimental results, q_t versus $t^{1/2}$ for different initial CR concentrations are shown in Fig. 6. It was observed from Table 2 and Fig. 6 that adsorption process was controlled by a multi-step process. The plots did not pass through the origin, indicating that intraparticle diffusion was not the only rate control step and there were some other mechanisms such as complexation or ion exchange were involved in the CR adsorption process. The R^2 values for intraparticle diffusion model were between 0.8263 and 0.9995 which were lower than pseudo-second-order kinetic model.

3.5. Isotherm analysis

Adsorptions isotherms describe the interactions between adsorbate and adsorbent. In this study, the Langmuir, Freundlich and Temkin isotherms were used to describe the properties of adsorption.

The Langmuir assumes that the sorption takes place at specific homogeneous sites within the adsorbent [28]. It is expressed as:

$$q_e = q_m K_a C_e / (1 + K_a C_e) \quad (5)$$

where q_e is the amount of CR adsorbed at equilibrium (mg/g), q_m is the maximum adsorption capacity of adsorbent (mg/g), C_e is the concentration of CR at equilibrium (mg/l) and K_a is the Langmuir constant (l/mg). q_m and K_a are calculated from the slopes and intercepts of the straight lines of plot of $1/q_e$ versus $1/C_e$. The values of q_m , K_a and the determination factor (R^2) for Langmuir model are given in Table 3.

The essential characteristics of the Langmuir equation can be expressed in term of a dimensionless separation factor, R_L , defined as [29].

$$R_L = 1 / (1 + K_a C_0) \quad (6)$$

Table 3
Isotherm constants for CR adsorption on SM at 25 °C

Isotherm	Values of parameters
<i>Langmuir</i>	
q_m (mg/g)	147.1
K_a (l/mg)	0.0605
R^2	0.9972
<i>Freundlich</i>	
K_F ((mg/g)(l/g) ⁿ)	13.8146
n	1.784
R^2	0.9361
<i>Temkin</i>	
A	0.7553
B	28.888
R^2	0.9830

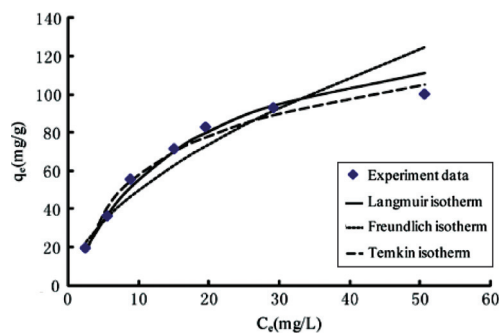


Fig. 7. Isotherm plots for CR adsorption on SM at 25 °C.

where C_0 is the initial concentration of the solution and K_a is the Langmuir's adsorption constant (l/mg).

The Freundlich isotherm assumes that the adsorption process takes place on heterogeneous surfaces and the equation can be written [30]:

$$q_e = K_F C_e^{1/n} \quad (7)$$

where K_F (mg/g (l/mg)^{1/n}) is the Freundlich constant which indicates the adsorption capacity and $1/n$ is the adsorption intensity. $1/n$ and K_F are calculated from the slopes and intercepts of the straight lines of plot of $\ln q_e$ versus $\ln C_e$. The values of K_F , n and the determination factor (R^2) for Freundlich model are given in Table 3.

Temkin isotherm assumes that the heat of adsorption of all the molecules increase linearly with coverage of the adsorbate molecules over adsorbent surface [31]. The Temkin isotherm has been used in the following form:

$$q_e = RT \ln(AC_0)/b \quad (8)$$

where A is the Temkin isotherm energy constant in l/g and B is the Temkin isotherm constant. B and A are calculated from the slopes and intercepts of the straight lines of plot of q_e versus $\ln C_e$. The values of A , B and the determination factor (R^2) for the Temkin model are given in Table 3.

Isotherm constants and isotherm plots for CR adsorption on SM at 25 °C are showed in Table 3 and Fig. 7, respectively. It can be seen that the experimental data fitted Langmuir isotherm better than the Freundlich

Table 4
Reported maximum adsorption capacities (q_{max} in mg/g) for CR obtained on low-cost adsorbents in the literature

Adsorbent	q_{max} (q_{max} in mg/g)	Reference
Coir pith	6.720	[24]
Activated red mud	7.080	[32]
Bagasse fly ash	11.88	[33]
Montmorillonite	12.70	[20]
Orange peel	14.00	[34]
Fungal biomass	14.16	[35]
Banana peel	18.20	[34]
Untreated sunflower stalks	34.26	[36]
Jute stick powder	35.7	[14]
Waste Fe(III)/Cr(III) hydroxide	44.00	[37]
Chitosan	81.23	[20]
Bamboo dust carbon	101.9	[38]
Spent mushroom	147.1	In this study
Bentonite	158.7	[23]
Coconut shell carbon	188.4	[38]
Rice husk carbon	237.8	[38]
Straw carbon	403.7	[38]

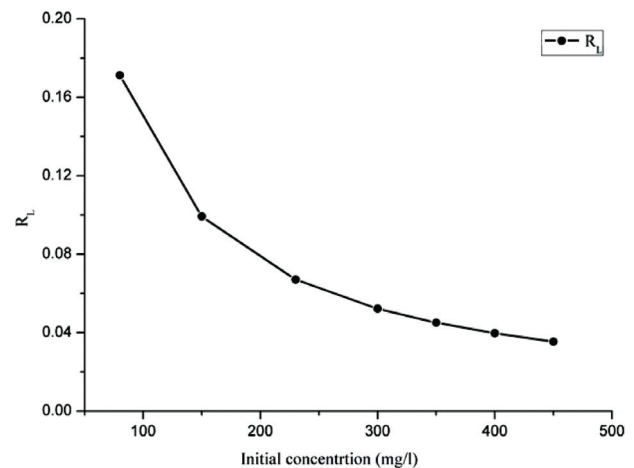


Fig. 8. The separation factor for CR adsorption on SM at 25 °C.

Table 5
The parameter R_L indicated the shape of isotherm

Value of R_L	Type of isotherm
$R_L > 1$	Unfavorable
$R_L = 1$	Linear
$0 < R_L < 1$	Favorable
$R_L = 0$	Irreversible

isotherm and the Temkin isotherm. This indicated that the adsorption of CR on SM was monolayer adsorption. The value of the determination factor (R^2) of Langmuir is 0.9972, which is higher than Freundlich (0.9361) and Temkin (0.9830). It is also can be seen from Table 2 that the maximum monolayer adsorption capacity (q_m) of SM for CR was 147.1 mg/g, which is lower than that of straw carbon, rice husk carbon, bentonite and coconut shell carbon, but higher than orange peel, Ca-bentonite, jute stick powder chitosan, montmorillonite and bagasse fly ash[0], as listed in Table 4.

As shown in Fig. 8, the value of R_L was in the range of 0–1 which confirms the favorable uptake of the CR (Table 5).

4. Conclusions

The present study investigated the adsorption of CR onto spent edible mushroom (*Tricholoma lobayense*). The amount of CR adsorbed decreased by increasing pH and increased with increasing initial concentration. The sorption equilibrium data fitted Langmuir isotherm and the maximum adsorption capacity was 147.1 mg/g. The kinetics of the adsorption followed the pseudo-second-order kinetic model. The adsorption of CR onto SM was also controlled by external mass transfer followed by intraparticle diffusion mass transfer. Edible mushroom grows in many countries in the world, so the spent edible mushroom can be easily acquired and it is feasible to use spent edible mushroom for removing Congo Red from wastewater in a commercial system.

Acknowledgements

This study was financially supported by National High Technology Research and Development Program (“863” Program) of China (2006AA06Z361), Science and Technology Supportive Project of Sichuan Province, China (2009SZ0204).

References

- [1] F. Meng and H. Yi, Application of different adsorbents on dyeing wastewater treatment, *Mater. Rev.*, 23 (2009) 69–73.
- [2] A.R. Gregory, S. Elliot and P. Kluge, Ames testing of direct black 3B parallel carcinogenicity, *J. Appl. Toxicol.*, 1 (1991) 308–313.
- [3] S.J. Allen, G. McKay and J.F. Porter, Adsorption isotherm models for basic dye adsorption by peat in single and binary component systems, *J. Colloid Interf. Sci.*, 280 (2004) 322–333.
- [4] O.J. Hao, H. Kim and P.C. Chiang, Decolorization of wastewater, *Crit. Rev. Environ. Sci. Technol.*, 30 (2000) 449–502.
- [5] B.H. Hameed and M.I. El-Khaiary, Sorption kinetics and isotherm studies of a cationic dye using agricultural waste: Broad bean peels, *J. Hazard. Mater.*, 154 (2008) 639–648.
- [6] B.H. Hameed, Spent tea leaves: A new non-conventional and low-cost adsorbent for removal of basic dye from aqueous solutions, *J. Hazard. Mater.*, 161 (2009) 753–759.
- [7] P. Janoš, H. Buchtová and M. Rýznarová, Sorption of dyes from aqueous solutions onto fly ash, *Water Res.*, 37 (2003) 4938–4944.
- [8] Renmin Gong, Shengxue Zhu, J.C. Demin Zhang, Shoujun Ni and R. Guan, Adsorption behavior of cationic dyes on citric acid esterifying wheat straw: kinetic and thermodynamic profile, *Desalination*, 230 (2008) 220–228.
- [9] Venkat S. Mane, Indra Deo Mall and V.C. Srivastava, Use of bagasse fly ash as an adsorbent for the removal of brilliant green dye from aqueous solution, *Dyes Pigments*, 73 (2007) 269–278.
- [10] B.H. Hameed, D.K. Mahmoud and A.L. Ahmad, Sorption of basic dye from aqueous solution by Pomelo (*Citrus grandis*) peel in a batch system, *Colloid. Surface. A.*, 316 (2008) 78–84.
- [11] B.H. Hameed and M.I. El-Khaiary, Removal of basic dye from aqueous medium using a novel agricultural waste material: pumpkin seed hull, *J. Hazard. Mater.*, 155 (2008) 601–609.
- [12] Lili Lian, L. Guo and C. Guo, Adsorption of Congo red from aqueous solutions onto Ca-bentonite, *J. Hazard. Mater.*, 161 (2009) 126–131.
- [13] R. Han, D. Ding, Y. Xu, W. Zou, Y. Wang, Y. Li and Lina Zou, Use of rice husk for the adsorption of congo red from aqueous solution in column mode, *Bioresour. Technol.*, 99 (2008) 2938–2946.
- [14] G.C. Panda, S.K. Das and A.K. Guha, Jute stick powder as a potential biomass for the removal of congo red and rhodamine B from their aqueous solution, *J. Hazard. Mater.*, 164 (2009) 374–379.
- [15] F.D. Ardejani, K. Badii, N.Y. Limaee, S.Z. Shafaei and A.R. Mirhabibi, Adsorption of Direct Red 80 dye from aqueous solution onto almond shells: effect of pH, initial concentration and shell type, *J. Hazard. Mater.*, 151 (2008) 730–737.
- [16] R. Malik, D.S. Ramteke and S.R. Wate, Adsorption of malachite green on groundnut shell waste based powdered activated carbon, *Waste Manage.*, 27 (2007) 1129–1138.
- [17] B.H. Hameed, A.A. Ahmad and N. Aziz, Isotherms, kinetics and thermodynamics of acid dye adsorption on activated palm ash, *Chem. Eng. J.*, 133 (2007) 195–203.
- [18] Flávio A. Pavan, Silvio L.P. Dias, Eder C. Lima and E.V. Benvenutti, Removal of Congo red from aqueous solution by anilinepropylsilica xerogel, *Dyes Pigments*, 76 (2008) 64–69.
- [19] M.K. Purkait, A. Maitim, S. DasGupta and S. De, Removal of congo red using activated carbon and its regeneration, *J. Hazard. Mater.*, 145 (2007) 287–295.
- [20] L. Wang and A. Wang, Adsorption characteristics of Congo Red onto the chitosan/montmorillonite nanocomposite, *J. Hazard. Mater.*, 147 (2007) 979–985.
- [21] S. Chatterjee, D.S. Lee, M.W. Lee and S.H. Woo, Enhanced adsorption of congo red from aqueous solutions by chitosan hydrogel beads impregnated with cetyl trimethyl ammonium bromide, *Bioresour. Technol.*, 100 (2009) 2803–2809.
- [22] H. Runping, H. Pan, Cai Zhaohui, Z. Zhenhui and T. Ming-sheng, Kinetics and isotherms of Neutral Red adsorption on peanut husk, *J. Environ. Sci.*, 20 (2008) 1035–1041.
- [23] E. Bulut, M. Özacar and İ. Şengil, Equilibrium and kinetic data and process design for adsorption of Congo Red onto bentonite, *J. Hazard. Mater.*, 154 (2008) 613–622.
- [24] C. Namasivayam and D. Kavitha, Removal of Congo Red from water by adsorption onto activated carbon prepared from coir pith an agricultural solid waste, *Dyes Pigments*, 54 (2002) 47–58.

- [25] S. Lagergren, Zur theorie der sogenannten adsorption gelöster Stoffe, *Kungliga svenska vetenskapsakademiens, Handl*, 24 (1898) 1–39.
- [26] Y.S. Ho and G. McKay, Sorption of dye from aqueous solution by peat, *Chem. Eng. J.*, 70 (1998) 115–124.
- [27] W.J. Weber and J.C. Morris, Kinetics of adsorption on carbon from solution, *J. Sanit. Eng. Div. Am. Soc. Civil Eng.*, 89 (1963) 31–60.
- [28] I. Langmuir, The adsorption of gases on plane surfaces of glass, mica and platinum, *J. Am. Chem. Soc.*, 40 (1918) 1361–1403.
- [29] K.R. Hall, L.C. Eagleton, A. Acrivos and T. Vermeulen, Pore- and solid-diffusion kinetics in fixed-bed adsorption under constant-pattern conditions, *I&EC Fundam*, 5 (1966) 212–223.
- [30] H. Freundlich, Über die adsorption in lösungen (Adsorption in solution), *Z. Phys. Chem.*, 57 (1906) 384–470.
- [31] M.J. Temkin and V. Pyzhev, Recent modifications to Langmuir Isotherms, *Acta Physicochim. USSR*, 12 (1940) 217–222.
- [32] A. Tor and Y. Cengelöglu, Removal of congo red from aqueous solution by adsorption onto acid activated red mud, *J. Hazard. Mater.*, 138 (2006) 409–415.
- [33] I.D. Mall, V.C. Srivastava, N.K. Agarwall and I.M. Mishra, Removal of congo red from aqueous solution by bagasse fly ash and activated carbon: kinetic study and equilibrium isotherm analysis, *Chemosphere*, 61 (2005) 492–501.
- [34] G. Annadurai, R.-S. Juang and D.-J. Lee, Use of cellulose-based wastes for adsorption of dyes from aqueous solutions, *J. Hazard. Mater.*, 92 (2002) 263–274.
- [35] Y. Fu and T. Viraraghavan, Removal of congo red from an aqueous solution by fungus *Aspergillus niger*, *Adv. Environ. Res.*, 7 (2002) 239–247.
- [36] W. Shi, X. Xu and G. Sun, Chemically modified sunflower stalks as adsorbents for color removal from textile wastewater, *J. Appl. Polym. Sci.*, 71 (1999) 1841–1850.
- [37] C. Namasivayam, R. Jeyakumar and R.T. Yamuna, Dye removal from wastewater by adsorption on waste Fe(III)/Cr(III) hydroxide, *Waste Manage.*, 14 (1994) 643–648.
- [38] N. Kannan and M. Meenakshisundaram, Adsorption of congo red on various activated carbons a comparative study, *Water, Air, Soil Pollut.*, 138 (2002) 289–305.